

Three-dimensional Simulation of Wet Combustion of Hydrogen-methane Mixture in the Annular Combustion Chamber of a Microturbine

A. Sohrabi and S. M. Mirsajedi[†]

Faculty of New Technologies and Aerospace Engineering, Shahid Beheshti University, Tehran, 1983969411, Iran

[†]Corresponding Author Email: m_mirsajedi@sbu.ac.ir

ABSTRACT

This study presents a three-dimensional simulation of wet combustion in the annular combustion chamber of a C30 microturbine using a hydrogen-methane fuel mixture. The research aims to minimize exhaust emissions, including nitrogen oxides (NO_x) and carbon monoxide (CO), and reduce fuel consumption. A partially premixed combustion model has been utilized to accurately simulate the combustion process within the chamber. The impact of steam addition (wet combustion) is also analyzed. The simulation employs the $k-\epsilon$ Realizable turbulence model and probability density function (PDF) for chemical reactions. The fuel mixture is adjusted by adding hydrogen in increments of 10%, resulting in a final composition of 40% hydrogen and 60% methane. With hydrogen's high heating value, the chamber temperature reaches 2376 K, significantly increasing NO_x and CO emissions. To control the temperature and maintain turbine operating conditions, the fuel mass flow rate is reduced by 35%, ensuring a consistent turbine inlet temperature. At this temperature, CO and CO₂ emissions decrease by 16% and 61%, respectively, while NO_x emissions increase due to hydrogen's flame characteristics. The introduction of humidity levels of 2.5%, 5%, 7.5%, and 10% in the inlet air reduces NO_x emissions by 68% in the case where the fuel mixture contains 10% hydrogen, with this reduction occurring at 10% humidity. Additionally, a 48% reduction in CO emissions was observed when the fuel mixture contained 40% hydrogen, and this reduction also occurred at 10% humidity. Wet combustion also enhances temperature uniformity in the chamber. These findings highlight the potential of hydrogen-methane mixtures with wet combustion to enable low-emission, efficient microturbines, supporting sustainable energy goals.

Article History

Received November 10, 2024

Revised February 8, 2025

Accepted February 9, 2025

Available online March 30, 2025

Keywords:

Turbulence

Chemical reactions

Premixed

Nitrogen oxides

Emission

1. INTRODUCTION

Microturbines, due to their simpler structure and higher efficiency, are considered a suitable alternative to traditional power generation systems by reducing emissions and allowing the use of clean fuels. With the ability to operate on a variety of fuels and reduce dependence on fossil fuels, these systems provide an effective solution for decentralized power generation and minimizing environmental impacts. In recent years, increasing concerns about climate change and the environmental impacts of fossil fuel combustion have driven researchers toward the development of advanced combustion technologies. These technologies aim to enhance energy efficiency, reduce harmful emissions such as nitrogen oxides (NO_x) and carbon dioxide (CO₂), and

ultimately mitigate environmental impacts. Key technologies in this domain include trapped vortex combustion (TVC), wet combustion, RQL (Rich-Burn, Quick-Mix, Lean-Burn) combustion, and exhaust gas recirculation (EGR).

Modern combustion technologies such as TVC, wet combustion, RQL, and EGR offer effective solutions to enhance the performance of combustion systems and reduce emissions. TVC systems, by rapidly mixing combustion products and reactants, not only lower emissions but also minimize pressure losses within the system (Haynes et al., 2006). Wet combustion, which introduces water into the combustion process (in the form of liquid, vapor, or direct injection), improves efficiency while significantly reducing pollutant production. The RQL technology, through its three stages of rich-burn,

NOMENCLATURE			
C_p	specific heat	S_{user}	user-defined source term
e	internal energy	S_h	heat generated from chemical reactions
f	mixture fraction	T	temperature
$\overline{f'^2}$	variance of the mixture fraction	t	time
\mathbf{v}	velocity vector	\mathbf{V}	velocity vector
V	velocity magnitude	V	velocity magnitude
Z	mass fraction of element	Z	mass fraction of element
ρ	density	ρ	density
σ_t	turbulent Prandtl number	σ_t	turbulent Prandtl number
$\bar{\tau}$	stress tensor	$\bar{\tau}$	stress tensor
μ_t	turbulent viscosity	μ_t	turbulent viscosity

quick-mix, and lean-burn combustion, effectively reduces nitrogen oxides and enhances energy efficiency, particularly in gas turbines and aircraft engines. Lastly, EGR technology recirculates a portion of exhaust gases back into the combustion chamber, lowering combustion temperatures and minimizing the formation of pollutants such as NO_x (Khosravy el_Hossaini, 2013).

Hydrogen is a clean fuel that produces only water vapor as a byproduct. However, extensive studies are still required concerning the amount of NO_x produced in systems that utilize hydrogen. Microturbines typically use CH₄ (methane) as fuel, and therefore, modifications in the combustion chamber are necessary to replace CH₄ with hydrogen. The level of fuel-air premixing in microturbines using hydrogen is crucial, as it significantly impacts the amount of NO_x produced (Therkelsen et al., 2006).

Therkelsen et al. (2009) investigated the performance of a gas microturbine fueled by hydrogen. They developed several injector models with nearly complete premixing. It was found that with almost complete premixing, the engine produced a higher amount of NO_x when operating on hydrogen compared to natural gas. A mixture of methane and hydrogen can be used without making significant modifications to combustion chambers designed to operate with methane. Reale et al. (2012) examined the emissions from a 100 kW microturbine. They used a mixture of hydrogen and methane containing 10% hydrogen. The results indicated that the hydrogen-methane blend had no significant impact on the production of CO and NO_x. Lu et al. (2022) simulated the effect of air distribution on the combustion characteristics of a micro gas turbine fueled by a hydrogen-methane mixture. When the premixed air was 30%, the combustion chamber's outlet temperature distribution was uniform, with an average outlet temperature of 1172 K. It was found that increasing the premixed air to 40% led to a rise in NO_x levels. Di Nardo et al. (2020) simulated the combustion performance of a microturbine fueled with CH₄, H₂, and CO₂. The results showed that the CO₂ content in the mixture should not exceed 50% by volume; otherwise, the performance significantly decreases. Shih and Liu (2014) conducted a computational study on the combustion of hydrogen-methane fuel blends in a model microturbine. The simulations were performed using a 3D compressible k- ϵ turbulence model and a probability density function for the chemical reaction. The results

indicated that with a fixed fuel mass flow rate, the flame temperature increases as the hydrogen fraction in the hydrogen-methane blend rises.

Du Toit et al. (2020) evaluated the performance and emission reduction of a small gas turbine through the combustion of H₂/CH₄/CO₂ fuel blends. The results showed that using this mixture leads to a reduction in CO and NO_x emissions. Meziane and Bentebbiche (2019) investigated the combustion of natural gas and hydrogen in a combustion chamber. The results showed that when the fuel mixture is injected at a constant mass flow rate, the outlet temperature increases, and the amount of NO_x produced also rises with the increase in hydrogen fraction. De Robbio (2017) analyzed the combustion in a gas microturbine burner using a hydrogen-natural gas mixture. The results showed that fuel containing 25% hydrogen leads to an increase in NO_x emissions. Serbin et al. (2022) simulated the combustion characteristics of a combustion chamber operating with a natural gas-hydrogen mixture using two different combustion models. The results showed that increasing the hydrogen fraction in the fuel leads to higher NO_x emissions, while CO emissions remain nearly constant. Funke et al. (2019) developed a low-emission micromix combustion system for use in industrial gas turbines fueled by hydrogen. Within the evaluated operational range of the combustion chamber, the combustion efficiency exceeded 99%. Carusotto et al. (2022) examined the combustion characteristics in a gas turbine burner using a hydrogen-methane fuel mixture. They concluded that when methane is blended with hydrogen, the peak temperature at the turbine inlet can increase by up to 800 K if no countermeasures are taken.

In a study by Nam et al. (2019), a numerical analysis was conducted on the effect of hydrogen composition in a gas turbine combustion chamber where the flow enters the combustion chamber in a partially premixed state. The results showed that as the hydrogen fraction increases, the flame becomes shorter and thicker, and its impact on the outer recirculation zone is minimized. Farokhipour et al. (2018) used an Eulerian-Lagrangian model to study the water spray injection process inside gas turbine combustion chambers. The results showed that water injection leads to a reduction in NO_x concentration. In a similar study, Reale and Sannino (2021) investigated the wet combustion of a hydrogen-methane mixture in a cylindrical combustion chamber. They injected steam at

up to 125% of the fuel mass flow rate. The results showed that steam injection leads to an increase in CO emissions. [Lellek et al. \(2017\)](#) experimented with the interaction of water spray with premixed natural gas flames. To achieve high water injection efficiency, ensuring complete evaporation of the water before the main heat release zone is essential. For this design objective, the water must be evenly distributed across the combustion section. [Pappa et al. \(2021\)](#) investigated the effect of water dilution to prevent flashback in a combustion chamber fueled by a hydrogen-methane mixture. The results showed that steam dilution helps reduce the hydrogen reaction rate, thereby preventing flashback. [Furuhata et al. \(2010\)](#) experimentally investigated the effect of steam addition on NO_x reduction in kerosene combustion. It was found that if steam is directly injected into the fuel spray, NO_x emissions decrease.

Recent studies on microturbine simulations have highlighted advancements in fuel flexibility, design optimization, and emission control. Investigations into biogas-fueled microturbines show reductions in NO_x emissions by 70% but highlight challenges such as increased CO emissions and reduced combustion efficiency, emphasizing the need for further optimization ([Bastani et al., 2025](#)). Additive manufacturing has enabled novel designs for combustion chambers, enhancing fuel-air mixing and reducing emissions while improving ignition performance ([Adamou et al., 2023](#)). Hydrogen combustion in reverse-flow combustors has been explored to achieve uniform thermal fields and lower NO_x emissions, though challenges remain with mixing and preheating effects ([Jamshidiha et al., 2024](#)). Multi-fuel compatibility and design modifications, such as optimized swirler vane angles, have shown potential to maintain high combustion efficiency while minimizing pollutant emissions ([Sher et al., 2024](#)). Studies on ammonia-hydrogen mixtures reveal viable temperature distribution comparable to methane combustion, reducing mechanical risks and supporting NO_x control ([Fafara, 2025](#)). Moreover, steam injection in ammonia-fed microturbines has demonstrated improved combustion efficiency and emission reductions, showcasing flexibility in power-to-heat ratios ([Fatehi et al., 2025](#)). Comprehensive models incorporating complex physico-chemical processes enable more accurate predictions of combustion behavior, aiding in the design of efficient and sustainable microturbines ([Bulat et al., 2024a, b](#)).

There are two main types of combustion chambers: cylindrical and annular. In microturbines, cylindrical combustion chambers are typically used due to their lower cost; however, this type tends to produce more emissions compared to the annular type. The selection and design of the combustion chamber are largely determined by the overall engine design and the need to use available space efficiently. In the annular combustion chamber design, an annular liner is concentrically installed within an annular casing. In many ways, this geometry represents an ideal design for a combustion chamber ([Lefebvre & Ballal, 2010](#)).

Modern combustion technologies such as TVC, RQL, and EGR have contributed to reducing emissions and

enhancing efficiency. However, the application of wet combustion in microturbine systems and its impact on hydrogen-methane fuel blends has been less extensively studied. A review of the existing literature reveals several critical research gaps. First, limited studies have focused on the wet combustion of hydrogen-methane mixtures in annular combustion chambers. Second, previous investigations have inadequately analyzed the role of humidification in reducing pollutants such as NO_x and CO, as well as improving combustion performance comprehensively. Finally, only a few efforts have been made to optimize combustion chambers for achieving both high efficiency and reduced emissions under varying operational conditions. This study aims to address these gaps by investigating the wet combustion of hydrogen-methane blends in annular microturbine combustion chambers.

In this study, the combustion chamber of the C30 microturbine was utilized for a detailed three-dimensional simulation of reactive flow. By employing a partially premixed combustion model, the fuel-air mixture entered the combustion chamber in a premixed state. The initial performance of the combustion chamber using pure CH₄ fuel was analyzed, and the simulation results were validated against the performance data of the C30 microturbine. To address the dual objectives of minimizing emissions and improving fuel efficiency, a methane-hydrogen fuel mixture was introduced, with hydrogen content incrementally increased to 40%. Furthermore, the effects of steam injection were investigated through wet combustion, demonstrating significant reductions in NO_x and CO emissions. An annular combustion chamber was utilized in this study to ensure optimal fuel-air mixing and effective heat distribution. This research uniquely combines hydrogen-enriched methane combustion with steam injection to achieve low-emission, efficient operation, providing valuable insights into optimizing microturbine performance for sustainable energy applications. The study also highlights the potential of wet combustion to enhance temperature uniformity, offering innovative solutions for the advancement of clean energy technologies.

2. PERFORMANCE SPECIFICATIONS OF MICROTURBINES

The C30 microturbine has low emissions and is used for combined heat and power (CHP) applications. This microturbine can operate with various gaseous, renewable, and liquid fuels, including natural gas, propane, flare gas, landfill gas, diesel, and kerosene. The combustion chamber of this microturbine is annular in design and is equipped with three injectors that inject the fuel-air mixture into the combustion chamber. The operational details of the C30 microturbine are provided in Table 1 ([Cameretti, 2020](#)).

The electrical efficiency of this microturbine is 26%. The exhaust temperature of the microturbine is 275°C (530°F), with an exhaust gas flow rate of 0.3 kg/s (0.68 lb/s).

Table 1 Performance Details of the Microturbine

Parameter	Value	Unit
Turbine inlet temperature	1173	K
Chamber outlet pressure	333747	pa
Pressure Ratio	3.45	-
Exhaust Mass flow	0.3	Kg/s
Electric efficiency	26	%
Speed	96000	rpm
Net Power output	30	kw

3. COMBUSTION CHAMBER GEOMETRY

The combustion chamber of the microturbine is an annular reverse-flow combustion chamber. The geometry of the microturbine's combustion chamber was created using SolidWorks software, based on the geometric information available in references (Chen et al., 2009, 2010; Abagnale et al., 2017). Figure 1 shows a view of the combustion chamber, along with the arrangement of the injector and the entry of the fuel-air mixture into the combustion chamber. The geometry of this combustion chamber differs from many other annular combustion chambers due to the unique arrangement of the microturbine components. The injectors of the studied combustion chamber are in the form of a tube with a diameter of 2.67 cm, equipped with a series of tangential and axial holes to enhance the mixing of fuel and air before entering the combustion chamber (Bolszo & McDonell, 2009). These injectors introduce the premixed fuel and air flow tangentially into the combustion chamber.

4. NUMERICAL METHODOLOGY

In this research, a steady-state three-dimensional simulation was conducted using the ANSYS Fluent software and the finite volume method. A pressure-based solver was employed with a coupled algorithm, as it is recommended for proper and fast convergence. The flow inside the combustion chamber was considered compressible and turbulent. The combustion modeling was performed using a partially premixed model, where a mixture of hydrogen and methane was burned with both dry and humid air inside the combustion chamber (Fluent, 2011; Patankar, 2018). Gravitational effects were neglected in this simulation. Convergence was achieved when the residuals of the combustion, momentum, and turbulence equations dropped below 10^{-5} , with 10^{-4} set as the convergence criterion for the continuity equation. Since the flow inside the liner is separate from the flow in the outer annulus, only the flow inside the liner was modeled to reduce computational cost and complexity.

4.1 Governing Equations

The three-dimensional form of the Navier-Stokes equations was used to perform the simulation. The governing equations of mass, momentum and energy conservation for turbulent reactive flows are as follows:

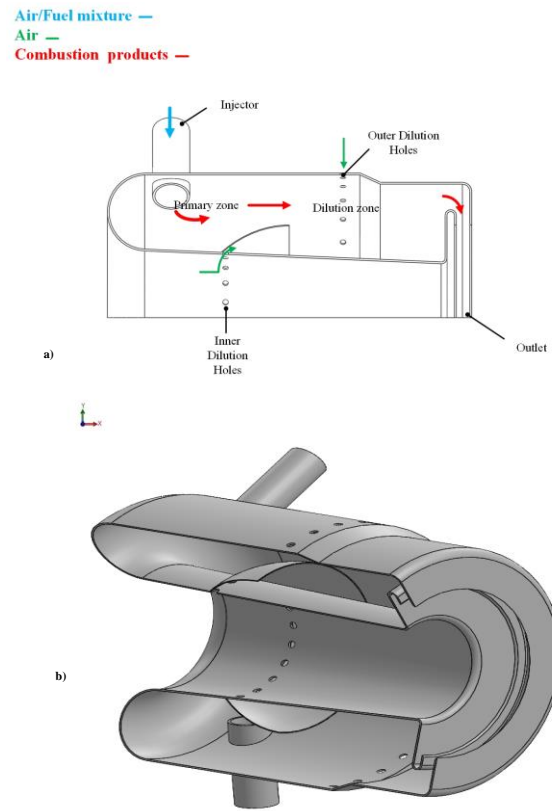


Fig. 1 a) Cross section of the annular combustion chamber showing the inlet and outlet of reactants and products, b) 3D annular combustion chamber geometry

The mass conservation:

$$\nabla \cdot (\rho \mathbf{V}) = 0 \tag{1}$$

Equation (1) represents the mass conservation equation for compressible and steady flows. In this equation, ρ represents density, and \mathbf{V} is the velocity vector.

The momentum conservation:

$$\nabla \cdot (\rho \mathbf{V} \mathbf{V}) = -\nabla p + \nabla \cdot (\bar{\boldsymbol{\tau}}) + \rho \mathbf{g} \tag{2}$$

The energy conservation:

$$\begin{aligned} &\nabla \cdot \left(\rho \mathbf{V} \left(h + \frac{V^2}{2} \right) \right) \\ &= \nabla \cdot \left(k_{eff} \nabla T - \sum_j h_j \mathbf{J}_j + \bar{\boldsymbol{\tau}}_{eff} \cdot \mathbf{V} \right) + S_h \end{aligned} \tag{3}$$

In Eq. (2), p represents the static pressure, $\bar{\boldsymbol{\tau}}$ is the stress tensor, and $\rho \mathbf{g}$ denotes the gravitational body force which was not considered in the current simulation. In Eq. (3), k_{eff} is the effective thermal conductivity and \mathbf{J}_j represents the diffusion flux of species j . The first three terms on the right-hand side of Eq. (3) correspond to energy transfer due to conduction, species diffusion and viscous dissipation respectively, while the term S_h represents the heat generated from chemical reactions

or any other heat source in the field.

The flow inside the microturbine combustion chamber is highly turbulent and swirling. To model the effects of turbulence in such flows, the k- ϵ and k- ω models are commonly used. The k- ϵ model is a two-equation model that offers good accuracy and stability for general modeling purposes. Due to its longstanding use and low computational cost, it remains one of the most widely employed turbulence models in engineering problems (Chen et al., 2017). In this study, the Realizable k- ϵ turbulence model was selected because of its ability to provide reliable numerical results for swirling flows and its significantly lower computational cost compared to the LES model (Fantozzi et al., 2009). In addition, the Realizable k- ϵ model was chosen for its improved accuracy in capturing swirling and recirculating flows, due to its enhanced formulations for turbulent viscosity and dissipation. Its efficiency and reliability for such flow characteristics make it well-suited for modeling the microturbine combustion chamber.

4.2 Combustion model

The partially premixed combustion model with a chemical equilibrium approach was used, offering efficient prediction of combustion products under fast reaction assumptions (Glanville et al., 2022; Wang et al., 2022). Partially premixed combustion systems involve flames where the oxidizer-fuel mixture is non-uniform. Under certain assumptions, thermochemistry can be reduced to a parameter called the mixture fraction. The mixture fraction, denoted by f , represents the mass fraction originating from the fuel stream and is expressed by Eq. (4). In other words, it describes the local mass fraction of fuel elements, both burnt and unburnt (C, H, etc.), across all species (CO₂, H₂O, O₂, etc.). In this combustion model, individual species equations are not solved; Instead, species concentrations are obtained from predicted mixture fraction fields. The interaction between turbulence and chemistry is calculated using an assumed shape of a probability density function (PDF). (Poinso & Veynante, 2005; Fluent, 2011).

The mixture fraction equation is :

$$f = \frac{Z_i - Z_{i,oxid}}{Z_{i,fuel} - Z_{i,oxid}} \quad (4)$$

Where Z_i is the mass fraction of element i , Z_{oxid} and Z_{fuel} represent the values for the oxidizer and fuel at the inlet stream, respectively.

In the partially premixed combustion model, the average mixture fraction equation is solved to capture the mixing of fuel and oxidizer (Eq. (5)). Based on the equal diffusion assumption, the average (density-weighted) mixture fraction equation is expressed as follows (De Robbio, 2017; Xiao et al., 2022):

$$\begin{aligned} \nabla \cdot (\rho \mathbf{V} \bar{f}) = \\ \nabla \cdot \left(\left(\frac{k}{C_p} + \frac{\mu_t}{\sigma_t} \right) \nabla \bar{f} \right) + S_m + S_{user} \end{aligned} \quad (5)$$

In Eq. (5), k is the thermal conductivity of the mixture, C_p is the specific heat of the mixture, σ_t is the turbulent Prandtl number and μ_t is the turbulent viscosity. The source term S_m is solely due to mass transfer to the gas phase from liquid fuel droplets or reacting particles. S_{user} represents any user-defined source term.

In addition to solving the mean mixture fraction \bar{f} , a conservation equation for the variance of the mixture fraction $\overline{f'^2}$ is also solved (Eq. (6)):

$$\begin{aligned} \nabla \cdot (\rho \mathbf{V} \overline{f'^2}) = \nabla \cdot \left[\left(\frac{k}{C_p} + \frac{\mu_t}{\sigma_t} \right) \nabla \overline{f'^2} \right] \\ + C_g \mu_t (\nabla \bar{f})^2 - C_d \rho \frac{\epsilon}{k} \overline{f'^2} + S_{user} \end{aligned} \quad (6)$$

Where $f' = f - \bar{f}$ and the values for the constants σ_t , C_g and C_d are 0.85, 2.86 and 2.0, respectively (Fluent, 2011; Medhat et al., 2021).

In this study, the Zimont correlation was employed to model the flame speed. The flame zone is characterized by solving an equation for the mean progress variable (\bar{C}), which varies between zero and one. The advancement of the flame front is captured by solving the transport equation for the mean progress variable, as described in Eq. (7) (Shan et al., 2022):

$$\begin{aligned} \nabla \cdot (\rho \mathbf{V} \bar{C}) = \\ \nabla \cdot \left(\left(\frac{k}{C_p} + \frac{\mu_t}{S C_t} \right) \nabla \bar{C} \right) + \rho S_c \end{aligned} \quad (7)$$

In this study, a mixture of methane and hydrogen was used as fuel. In the simulation, the combustion process was analyzed under two conditions: first with pure air and then with humid air, to evaluate the effects of steam injection on combustion performance and emissions. The resulting reaction involves 20 species, which are: H₂, CH₄, O, N₂, O₂, H₂O, CO, CO₂, OH, H, HO₂, H₂O₂, HONO, HCO, CHO, HOCO, O₃, HCOOH, CH₂O, HNO₂. The thermal and prompt NO_x mechanisms were also adopted to predict the amount of NO_x produced (De Soete, 1975; Caldeira-Pires et al., 2000).

4.3 Boundary Conditions

Using the microturbine's performance parameters, the boundary conditions were applied for the full load case with pure methane as fuel. The injectors were modeled as nozzles that inject a premixed fuel-oxidizer mixture into the combustion chamber. The combustion chamber walls were assumed to be stationary and impermeable with no-slip boundary conditions. The chamber's inlets, including injectors and dilution holes, were modeled as velocity inlets, while the outlet was set as a pressure outlet. The detailed boundary conditions for the full load case with pure methane can be seen in Table 2.

5. MESH INDEPENDENCE ANALYSIS

The combustion chamber geometry was meshed with different numbers of elements. In this study, the computational domain represents one-third of the annular combustion chamber, selected to reduce computational

Table 2 Boundary conditions

Parameter (Unit)	Value
Fuel mass flow (kg/s)	0.0032
Species Mean Mixture Fraction at the injector inlet	0.0315
The temperature of the fuel-air mixture from the injector inlet (K)	870
Air mass flow (kg/s)	0.31
Outlet pressure (KPa)	333

cost while maintaining accuracy and symmetry in the simulation results. This simplification is justified by the periodicity of the combustion chamber, allowing the use of periodic boundary conditions for accurate modeling of the entire domain. Due to the complex geometry of the model, an unstructured mesh was utilized. Structured meshes are typically employed for simpler geometries, whereas unstructured meshes are more suitable for complex geometries. The elements within the mesh are a combination of tetrahedral, wedge, and pyramidal elements.

For the boundary layer, wedge (Wed6) or prism elements are commonly used. These elements, due to their wedge-shaped or prismatic structure, are highly suitable for modeling sharp gradients and boundary layers. They are typically employed near solid surfaces (such as walls) to better capture steep variations in parameters like velocity and temperature within the boundary layers.

To enhance the accuracy of flow and combustion simulations in the combustion chamber, finer mesh resolutions were applied in critical regions near dilution holes, injectors, and the outlet. This approach aims to achieve more precise modeling of turbulent phenomena, fuel-air mixing, and the distribution of velocity and temperature gradients.

Four mesh types were generated with 1,315,425, 1,592,667, 1,792,334, and 1,890,456 elements, by adjusting the mesh size factor. Figure 2 shows an example of the generated mesh for the combustion chamber under study.

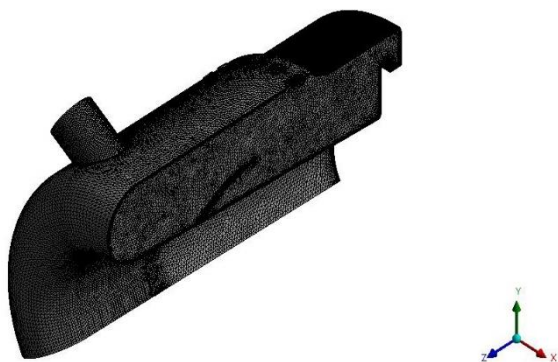


Fig. 2 Mesh of combustion chamber

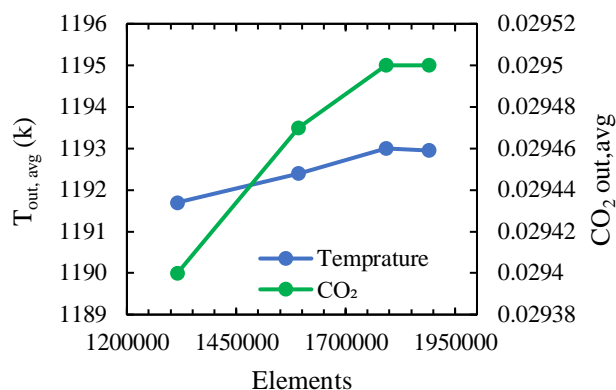


Fig. 3 Variation of temperature and CO₂ emissions with increasing mesh elements

The grid independence test was conducted using the four different mesh types created in ANSYS Fluent, applying the same initial and boundary conditions. Since the average outlet temperature and CO₂ emission levels are key parameters in evaluating combustion performance, they were selected as criteria for the mesh study. As shown in Fig. 3, the variations in these parameters become negligible as the number of mesh elements increases, indicating a trend toward stability. This suggests that increasing the number of mesh elements has an insignificant impact on the computations. To strike a balance between computational efficiency and accuracy, the mesh with 1,792,334 elements was selected for further calculations.

6. VALIDATION

The performance with pure CH₄ fuel at full load is considered as the baseline case for validation of the results. The best data for validation are the exhaust temperature and the emission levels. Table 3 compares the exhaust temperature, NO_x and CO emissions obtained from the simulation with the official data provided by the C30 microturbine manufacturer (Chen et al., 2010; Abagnale et al., 2017; Cameretti, 2020).

The comparison of experimental and numerical results shows that the temperature difference at the exit is only 20 K, corresponding to an error of 1.7%. Additionally, the NO_x results indicate a minimal error of 4%. However, the simulation results show a discrepancy in CO concentration compared to experimental data, likely due to limitations in the combustion model. Achieving accurate predictions of this pollutant is challenging in simulations, as all

Table 3 Comparison of experimental data with numerical simulation results

Parameter	Experimental data	Numerical data
T _{out,ave} (K)	1173	1193
CO at 15% O ₂ (ppm)	40	50.9
NO _x at 15% O ₂ (ppm)	9	9.4

Table 4 Gas fuels with different compositions

Case	Mass % CH ₄	Mass % H ₂	LHV (MJ/kg)	Volume % CH ₄	Volume % H ₂	Energy % H ₂
1	100%	0%	50.02	100%	0%	0%
2	90%	10%	56.996	82.16%	17.84%	21.06%
3	80%	20%	63.99	64.33%	35.67%	37.51%
4	70%	30%	70.98	46.5%	53.5%	50.73%
5	60%	40%	77.98	28.67%	71.33%	61.54%

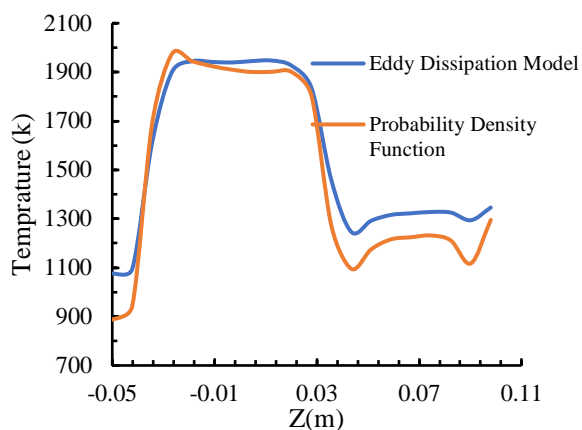


Fig. 4 Temperature distribution comparison along the combustion chamber using the PDF model from this study and the EDM model from reference (Sohrabi & Mirsajedi, 2024)

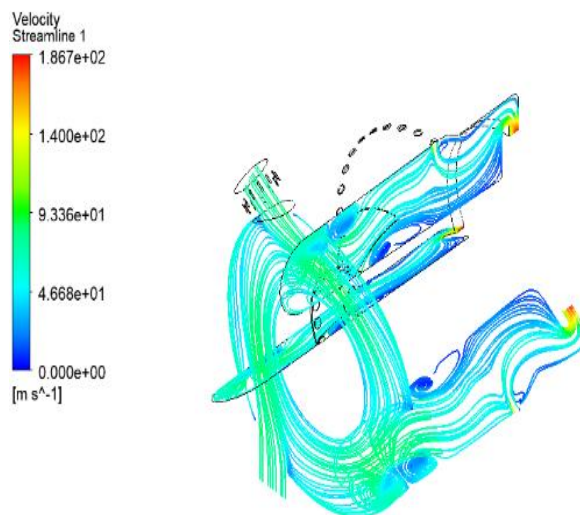


Fig. 5 Velocity streamlines inside the combustion chamber

combustion reactions must be considered. To improve accuracy, more complex mechanisms, such as the Eddy Dissipation Concept Model, should be applied, though this would increase computational costs and complexity.

The temperature distribution along the combustion chamber, obtained using the Probability Density Function combustion model, was compared with reference (Sohrabi & Mirsajedi, 2024) in Fig. 4. The reference (Sohrabi & Mirsajedi, 2024) employed the Eddy Dissipation Model (EDM) for simulating reactive flow. As observed, the temperature behavior along the chamber is approximately consistent. However, the results indicate that the EDM overpredicts the temperature compared to the present model. Consequently, the utilization of the PDF combustion model has improved the accuracy of the results.

7. RESULT AND DISCUSSIONS

Hydrogen is a clean fuel that produces only water vapor as a byproduct, making the study of hydrogen-methane combustion mixtures highly beneficial. Hydrogen has a density of approximately 0.0898 kg/m³ and a lower heating value (LHV) of around 121.2 MJ/kg. Table 4 provides details of the fuel mixtures used in this simulation. As the hydrogen mass percentage increases from 0% to 40% across the cases, the LHV rises from 50.02 MJ/kg to 77.98 MJ/kg, demonstrating hydrogen's high energy density. Similarly, the energy contribution of increases significantly, reaching 61.54% in Case 5. This trend is accompanied by a decrease in methane's volume

percentage and an increase in hydrogen's volume percentage.

7.1 Streamlines and Temperature Contour

The fuel-air mixture is injected tangentially from the injectors into the main combustion zone, causing the flow to move in the circumferential direction of the combustion chamber, facilitating optimal combustion. Additionally, due to the flow characteristics and the appropriate geometry of the chamber, the flame will remain stable. Figure 5 shows the velocity streamlines inside the combustion chamber. An inner liner is present, helping to keep the main flow centered. The location of the dilution holes is also shown, which are used to complete combustion and control the exhaust temperature.

In Fig. 6, the temperature field for pure methane combustion is shown in Kelvin in two different planes. When the fuel-air mixture is injected into the primary combustion zone through the injectors, efficient combustion occurs, resulting in a stable flame. As combustion progresses within the primary zone, the chamber temperature increases to approximately 1900 K. The swirling flow then moves toward the outlet, entering the dilution zone, where additional air is injected into the combustion products to regulate the temperature for turbine entry. The outlet temperature, as observed, is highly uniform, which enhances the durability of the turbine blades.

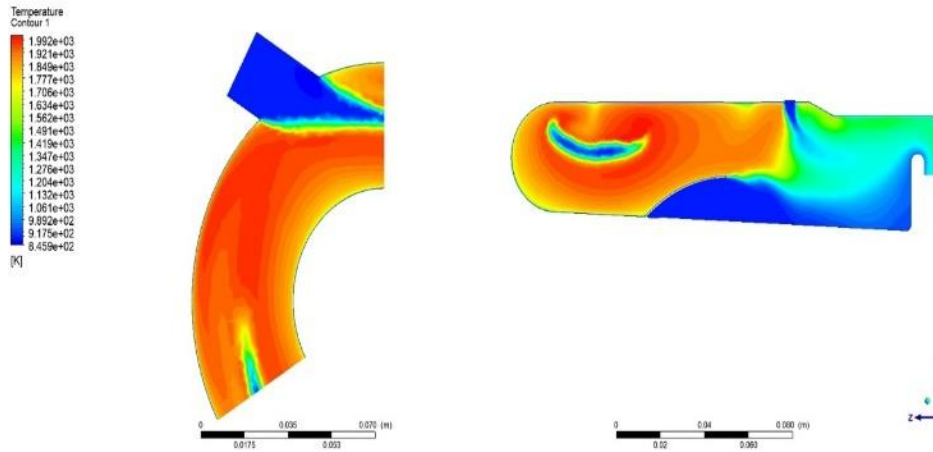


Fig. 6 Temperature contour in combustor

7.2 The Effect of Hydrogen Addition at a Constant Fuel Mass Fraction

The combustion of a hydrogen-methane mixture was initially studied at a constant fuel mass fraction. In all cases presented in Table 4, the fuel-air mixture was injected into the primary combustion zone through an injector at a velocity of 77 m/s. As hydrogen was added to methane, the density of the mixture decreased due to hydrogen's significantly lower density compared to methane. Consequently, the reduction in mixture density led to a decrease in the fuel mass flow rate entering the combustion chamber. When pure methane was used, the fuel mass flow rate was 0.0032 kg/s, and This value decreased by approximately 3% with each 10% increase in hydrogen content in the fuel. For instance, the mass flow rate decreases by 11% when the mixture is composed of 40% hydrogen.

7.2.1 Temperature Distribution Trends for Different Fuel Compositions

Figure 7 shows the temperature distribution along the axial direction of the combustion chamber with different fuel components at a constant fuel mass fraction. The temperature distribution is examined along a line from the injector inlet to the outlet of the chamber. The location of this line is determined by averaging the inner and outer diameters of the chamber. In the case of using pure methane, the temperature in the chamber is initially around 900 K, then rises to approximately 2000 K before gradually decreasing in the dilution zone due to the injection of additional air. With the addition of hydrogen to methane, the temperature along the chamber increases due to the higher heating value of the mixture, reaching a maximum of approximately 2376 K in the primary combustion zone. As previously discussed, when the fuel mixture comprises 40% hydrogen, the mass flow rate of the fuel entering the combustion chamber decreases by only 11%. However, the elevated heating value of hydrogen leads to a continued rise in the chamber's temperature.

With the increase in the temperature generated in the combustion chamber, the turbine inlet temperature also

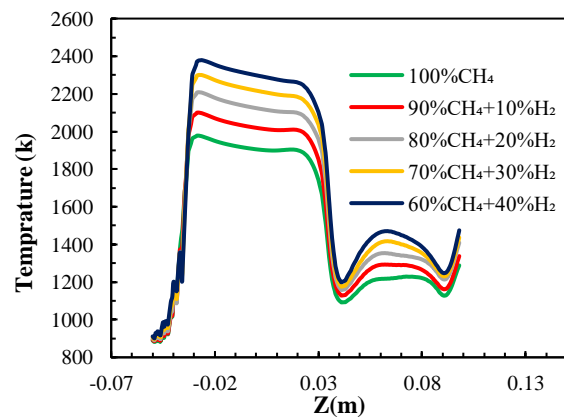


Fig. 7 Temperature distribution along the chamber at constant fuel mass fraction

rises. For instance, when the mixture consists of 40% hydrogen, the turbine inlet temperature increases to approximately 1364.9 K.

7.2.2 Effect of Hydrogen Addition on Emissions at Constant Fuel Mass Fraction

The concentration of NO_x and CO is highly dependent on the temperature (Lefebvre & Ballal, 2010). As shown in Fig. 8, NO_x production consistently increases with rising temperature and decreases as the temperature drops. However, the behavior of CO emissions with respect to temperature is different, as shown in Fig. 9. CO levels decrease within the temperature range of 1500 to 1850 K, but increase as the temperature rises beyond this range. Therefore, for the combustion chamber to achieve the lowest emissions, it should operate within the temperature range of 1700 to 1900 K (Lefebvre & Ballal, 2010). As observed in Fig. 7, adding hydrogen to the fuel causes the temperature to exceed 2000 K, which results in an increase in both NO_x and CO emissions. Figure 10 illustrates the production levels of NO_x and CO at different hydrogen mass percentages. It can be seen that increasing the hydrogen content in the fuel mixture leads to higher emissions of both CO and NO_x.

Table 5 Comparison of CO and NOx Emissions for Different Fuel Compositions with Percentage Increase Relative to Pure Methane

Fuel Composition	CO (ppm)	Percentage Increase in CO Relative to Pure Methane (%)	NOx (ppm)	Percentage Increase in Nox Relative to Pure Methane (%)
90 CH ₄ + 10 H ₂	129	153.5	37.8	302.1
80 CH ₄ + 20 H ₂	258	406.8	146.6	1459.6
70 CH ₄ + 30 H ₂	461	805.3	391.8	4067.0
60 CH ₄ + 40 H ₂	705	1285.3	802.9	8443.6

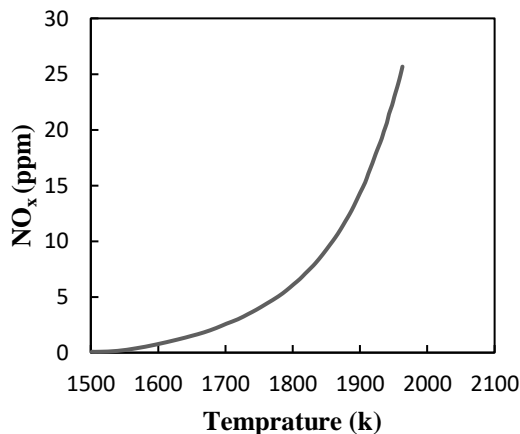


Fig. 8 NOx concentration at different temperatures (Lefebvre & Ballal, 2010)

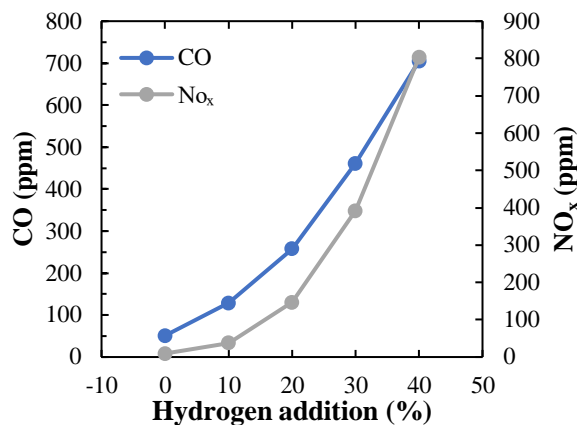


Fig. 10 NOx and CO pollutant concentrations as a function of hydrogen addition at a constant fuel mass fraction

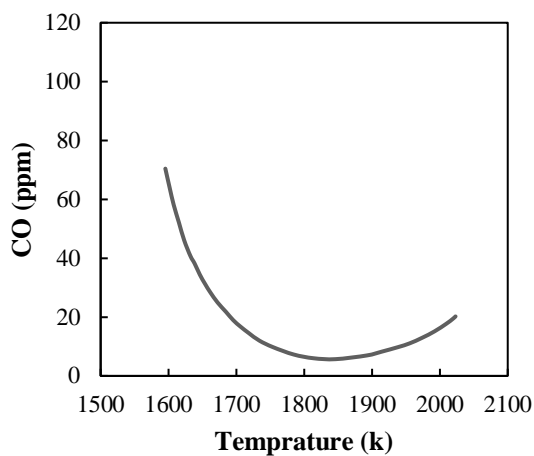


Fig. 9 CO concentration at different temperatures (Lefebvre & Ballal, 2010)

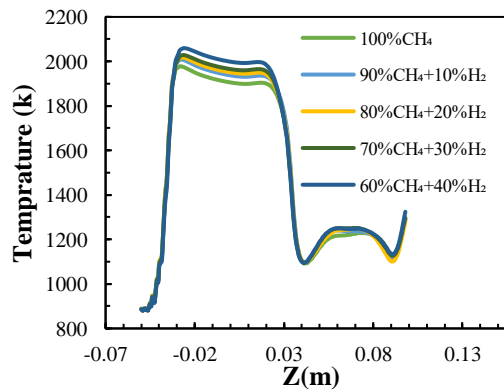


Fig. 11 Temperature distribution along the chamber at constant turbine inlet temperature

Table 5 provides a comparison of CO and NOx emissions for various fuel compositions containing different proportions of CH₄ and H₂. The table also highlights the percentage increase in CO and NOx emissions relative to pure methane. As the hydrogen content increases in the fuel mixture, both CO and NOx emissions exhibit a significant rise.

7.3 The Effect of Hydrogen Addition at a Constant Turbine Inlet Temperature

In the previous section, it was observed that adding hydrogen at a constant fuel mass fraction ultimately leads to an increase in harmful pollutants such as CO and NOx.

Due to the differences in the combustion properties of methane and hydrogen, the combustion performance of the chamber should be evaluated at a constant turbine inlet temperature (Therkelsen et al., 2009). The fuel input to the chamber was reduced to achieve the same turbine inlet temperature. Again, the fuel with different compositions, as shown in Table 4, was injected into the chamber. Figure 11 shows the temperature distribution along the chamber at a turbine inlet temperature of 1193 K. As seen, with the increase in the hydrogen share in the mixture, the temperature in the primary combustion zone rises even further compared to the use of pure methane, reaching a maximum of 2060 K. However, all cases indicate that as

Table 6 Reduction in Fuel Mass Flow and CO₂ Mass Fraction for Various Methane-Hydrogen Fuel Compositions Relative to Pure Methane

Fuel Composition	Fuel Mass Flow (kg/s)	Percentage Reduction in Fuel Mass Flow Relative to Pure Methane (%)	CO ₂ (Mass Fraction)	Percentage Reduction in CO ₂ Relative to Pure Methane (%)
90 CH ₄ + 10 H ₂	0.00286	10.63	0.0234	20.68
80 CH ₄ + 20 H ₂	0.0025	21.88	0.0187	36.61
70 CH ₄ + 30 H ₂	0.0023	28.13	0.0147	50.17
60 CH ₄ + 40 H ₂	0.0021	34.38	0.0115	61.02

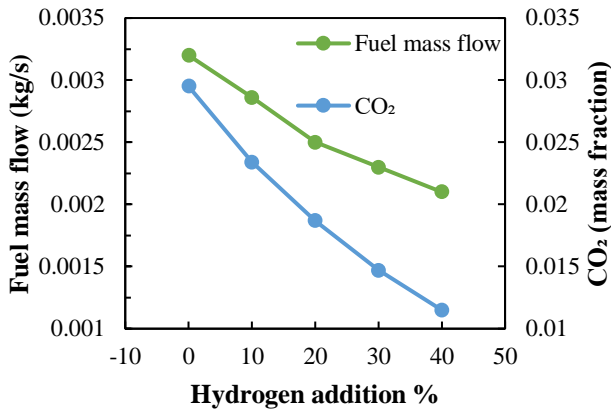


Fig. 12 Fuel flow rate and CO₂ mass fraction at the outlet for various hydrogen additions to the fuel, while maintaining a constant turbine inlet temperature

the flow enters the dilution zone, the temperature behavior becomes uniform and ultimately reaches 1193 K at the chamber exit. The reason for the temperature rise in the primary combustion zone is the different combustion properties of hydrogen and methane, including reaction rates, flame speed and flame temperature (Therkelsen et al., 2009).

7.3.1 Fuel Consumption and Emissions at Constant Turbine Inlet Temperature

Figure 12 illustrates the fuel consumption and CO₂ emissions at the outlet as the hydrogen fraction in the fuel increases. Both fuel input and CO₂ emissions decrease with the rise in hydrogen content. Compared to combustion with a constant fuel mass fraction, the reduction in fuel consumption and CO₂ emissions is more significant, as the fuel mass flow rate is reduced to maintain a constant turbine inlet temperature across different conditions, leading to a decrease in methane intake. When the fuel mixture contains 40% hydrogen, fuel consumption decreases by approximately 35%, and CO₂ emissions are reduced by around 61%.

Table 6 presents the reduction in fuel mass flow and CO₂ mass fraction for various methane-hydrogen fuel compositions compared to pure methane. As the hydrogen content in the fuel increases, a consistent reduction in both fuel mass flow and CO₂ mass fraction is observed.

The results of the previous section indicated that NO_x and CO emissions are highly dependent on the combustion temperature. Therefore, assessing these emissions at a

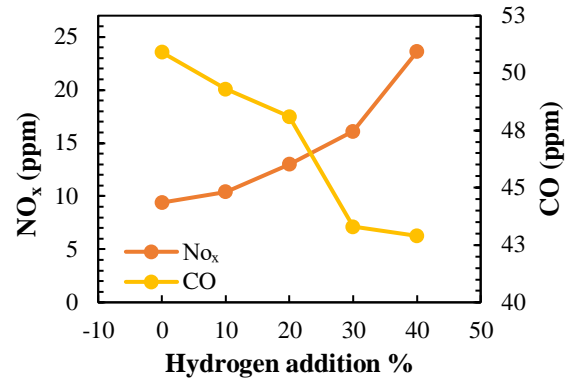


Fig. 13 CO and NO_x emissions as a function of hydrogen addition at a constant turbine inlet temperature

constant turbine inlet temperature is particularly useful. In Fig. 13, the variation in CO and NO_x emissions with increasing hydrogen content in the fuel mixture is presented. The NO_x levels gradually rise as the hydrogen fraction increases, reaching a maximum of 23.6 ppm. This increase in NO_x is directly related to the rise in temperature (Lefebvre & Ballal, 2010). However, CO emissions decrease with higher hydrogen fractions, dropping to a minimum of 42.9 ppm. This reduction in CO is due to the reduced methane content in the fuel and the decrease in the fuel mass flow rate. Moreover, since hydrogen combustion does not produce carbon-based emissions, no carbon monoxide is formed (Meziane & Bentebbiche, 2019).

7.4 Wet Combustion of Hydrogen and Methane Mixture

Water, due to its high specific heat capacity and latent heat of vaporization, absorbs heat within the combustion chamber, leading to a reduction in temperature and a decrease in NO_x emissions (Banerjee et al., 2021). Adding hydrogen to methane increases flame temperature and speed, which in turn leads to higher NO_x emissions (Therkelsen et al., 2006; Shih & Liu, 2014). It was observed that as the hydrogen fraction in the fuel increases, NO_x emissions rise even when the turbine inlet temperature remains constant. Injecting water and using humid air can effectively reduce pollutants such as NO_x. Therefore, wet combustion with different fuel mixtures was examined. Humid air with moisture levels of 2.5%, 5%, 7.5%, and 10% was introduced into the combustion chamber.

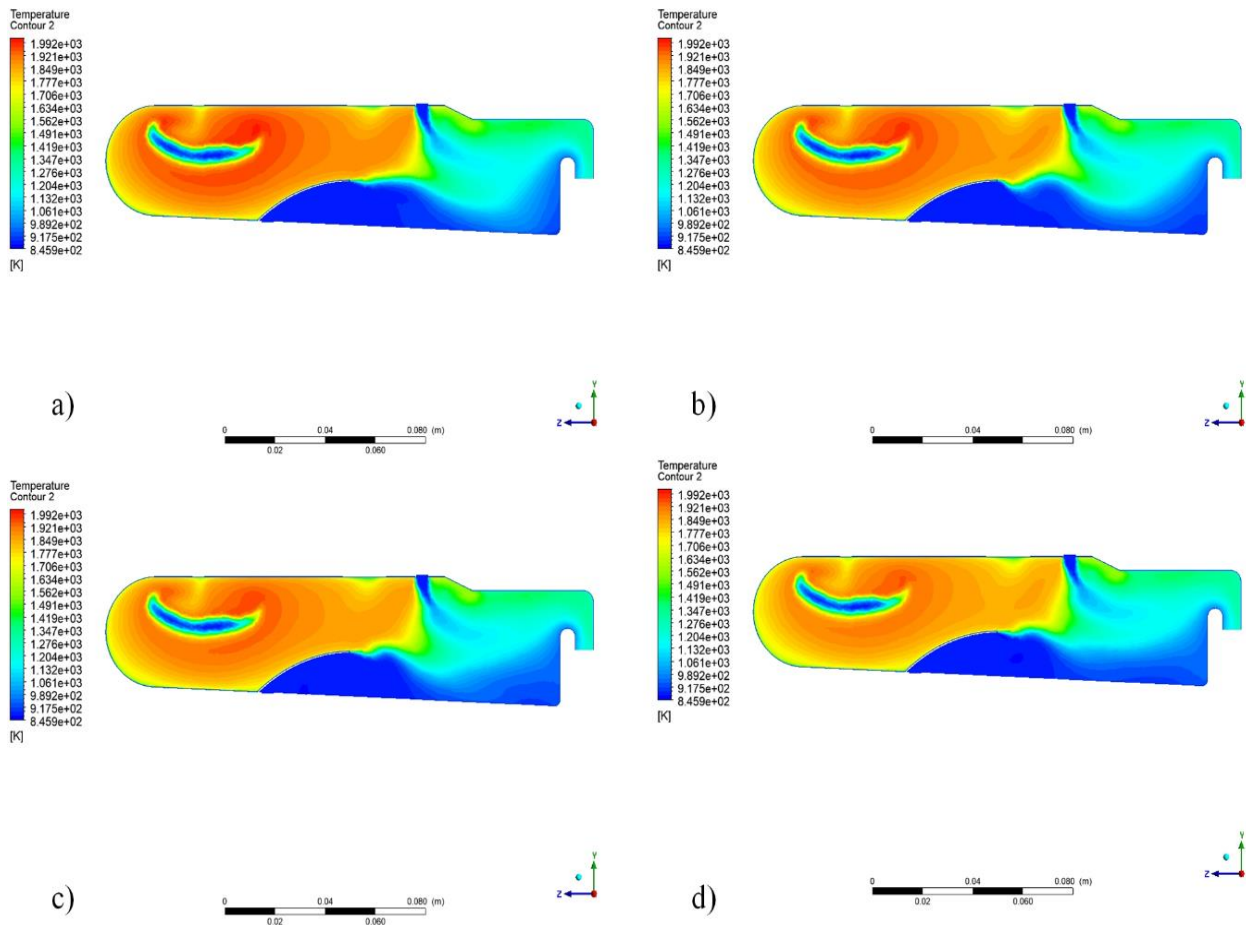


Fig. 1 Wet combustion temperature contour with pure methane fuel a) 2.5% Humidity, b) 5% Humidity, c) 7.5% Humidity, d) 10% Humidity

7.4.1 Wet Combustion of Methane in the Annular Combustion Chamber

Initially, wet combustion of pure methane was studied. In Fig. 14, the temperature field in the combustion chamber with varying humidity levels using pure methane fuel is shown. The injection of water vapor improves the temperature distribution in the primary zone of the chamber and reduces the intensely hot regions. This is highly effective in reducing pollutant emissions.

When steam is injected into the combustion chamber, it absorbs a significant amount of heat due to its high specific heat capacity, thereby reducing the maximum combustion temperature. The presence of moisture in the air also lowers the concentrations of oxygen and nitrogen (Bouam et al., 2008).

Under dry air conditions, the maximum temperature within the combustion chamber reaches 2016.1 K. Humidity, however, reduces the maximum temperature inside the combustion chamber. For instance, when the inlet air has a humidity level of 10%, the peak temperature decreases to 1950.5 K, indicating a 3.2% temperature drop compared to pure air.

Figure 15 shows the temperature distribution along the chamber, assuming wet combustion with pure methane fuel. Using humidified air lowers the flame temperature.

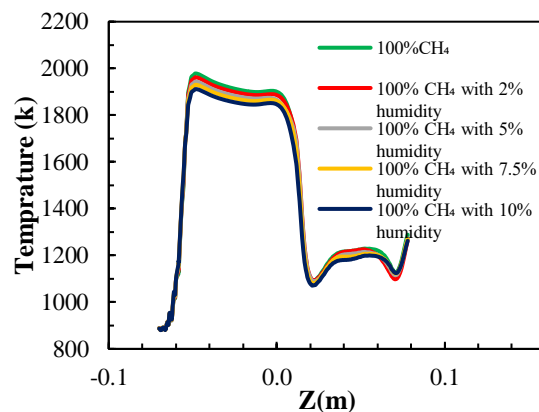


Fig. 15 Temperature distribution along the combustion chamber with varying humidity levels in pure methane combustion

As observed in Fig. 15, the primary CH_4 combustion zone experiences a temperature drop with increased humidity in the inlet air. In contrast, in the dilution zone, temperature behavior shows minimal change with added humidity, ensuring that increased humidity in the inlet air does not significantly decrease the turbine inlet temperature.

Table 7 Results from wet combustion of pure methane

Case	Percentage of humidity (%)	TIT (K)	NO _x (ppm)	CO (ppm)
	0	1193	9.4	50.9
	2.5 %	1187.8	6.7	45.5
1 a	5 %	1178.8	4.54	40.3
	7.5 %	1174.4	3.34	37
	10 %	1163.6	2.27	32.9

Table 7 presents the results of wet combustion using pure methane. The mass flow rate of the fuel input is 0.0032 kg/s. As the air humidity increases, the turbine inlet temperature decreases. For instance, with 10% humidity in the incoming air, the inlet temperature of the chamber drops to 1163.6 K, resulting in a 2.4% reduction in turbine inlet temperature. Since steam is introduced instead of water, the temperature drop remains moderate.

According to Table 7, a decrease in temperature leads to a reduction in NO_x emissions. When pure methane is used, NO_x emissions reach 9.4 ppm; however, when the inlet air contains 10% humidity, this value decreases to 2.27 ppm, showing that humidified air can achieve a 76% reduction in NO_x emissions without causing a significant drop in temperature. Many studies indicate that injecting steam or water into the combustion chamber typically increases CO emissions (Lefebvre & Ballal, 2010; Reale & Sannino, 2021; Reale, 2022). However, a small premixed amount of steam injection can reduce CO emissions. As seen in the table 7, increasing air humidity consistently decreases CO emissions, with the lowest CO emissions observed at 10% air humidity.

7.4.2 Wet Combustion of a methane-hydrogen mixture in the Annular Combustion Chamber

The use of hydrogen led to a reduction in carbon oxide emissions but increased NO_x emissions due to the higher flame temperature. As discussed in the previous section, increasing the hydrogen content in the fuel raises the temperature in the primary combustion zone. Figure 14 also shows that the dominant effect of air humidity is on the primary combustion zone. As a result, air humidification can prevent this temperature increase in the primary zone when using a hydrogen-methane mixture. Since the majority of NO_x emissions are formed in the primary zone of the combustion chamber, the resulting temperature reduction in this area is highly beneficial.

Table 8 presents the details of the wet combustion of a methane-hydrogen mixture with different fuel compositions and humidity levels. In each of the following cases, combustion was conducted with dry air and humidity levels of 2.5%, 5%, 7.5%, and 10%. In case 2a, the mass flow rate of fuel consumption is 0.00286 kg/s, and as the hydrogen content in the fuel increases, the mass flow rate of the fuel decreases, reaching a minimum of 0.0021 kg/s. With an increase in air humidity, the turbine inlet temperature decreases, leading to a reduction in NO_x emissions. Additionally, it is observed that the CO emissions also decrease with higher humidity levels.

According to Fig. 9, it was observed that CO

emissions are highly dependent on temperature. Specifically, if the temperature drops below 1850 K, the production of CO emissions increases. However, since steam is used and the fuel-air mixture is pre-mixed before entering the chamber, the temperature drop is minimal. In cases 3a, 4a, and 5a, similar behavior is observed in the turbine inlet temperature and the emissions of CO and NO_x. In all cases, it is evident that the highest level of emissions occurs when using dry air, while increasing the humidity level in the air leads to a reduction in these emissions. Additionally, it is observed that the temperature drop with increased air humidity is not dependent on the fuel composition. For example, in case 2a, when the air entering the chamber has 10% humidity, the turbine inlet temperature is 1167.1 K. Similarly, in case 5a, when the air has 10% humidity, the turbine inlet temperature or the outlet temperature of the combustion chamber is also 1167.1 K.

According to the table 8, the highest level of NO_x is observed in case 5a, reaching 23.6 ppm, as the fuel consists of 40% hydrogen. Furthermore, in this case, the lowest level of CO emissions is observed at 10% humidity, amounting to 26.5 ppm. In case 2a, when the air has 10% humidity, the lowest NO_x emissions are produced, while the highest level of CO emissions occurs, as 90% of the fuel is composed of CH₄.

Adding hydrogen to methane generally reduces the effective residence time in the combustion chamber. This reduction is due to the increased rate of chemical reactions, higher flame speed, and elevated combustion temperature. However, the precise effect depends on the combustion chamber design, flow conditions, and the fuel-air mixing ratio. The increase in NO_x emissions is strongly temperature-dependent, as higher temperatures lead to higher NO_x formation, and reducing residence time alone is insufficient to mitigate NO_x production.

For CO emissions, while a reduction in residence time can potentially result in incomplete combustion, the addition of hydrogen and steam prevents significant temperature drops. As a result, complete combustion is achieved, leading to reduced CO emissions.

The combustion simulation is performed using pure methane at an equivalence ratio of 0.18, representing lean combustion conditions. The formation of NO_x is primarily influenced by temperature rather than the equivalence ratio. Adding hydrogen increases the combustion temperature while reducing the equivalence ratio under both constant fuel mass fraction and constant turbine inlet temperature scenarios.

In terms of CO emissions, a lower equivalence ratio could theoretically reduce temperature due to incomplete combustion. However, since no significant temperature drop is observed, CO emissions are reduced. Furthermore, the reduction in methane content in the fuel mixture also contributes to the decreased CO emissions.

Based on the results of Table 8, it is possible to reduce NO_x emissions by up to 68% and CO emissions by up to 48% compared to the baseline by using humidified combustion of the hydrogen-methane mixture. In case 5a,

Table 1 Results of wet combustion of methane-hydrogen mixture with different fuel compositions and moisture levels

Case	Fuel composition and mass flow of fuel	Humidity (%)	TIT (K)	NO _x (ppm)	CO (ppm)
2 a	90 CH ₄ + 10 H ₂ 0.00286 (kg/s)	0	1193	10.4	49.3
		2.5	1185.8	7.74	44.6
		5	1179.7	5.59	39.7
		7.5	1174.5	4.36	36.4
		10	1167.1	3.05	32.4
3 a	80 CH ₄ + 20 H ₂ 0.0025 (kg/s)	0	1193	13	48.1
		2.5	1189.6	9.95	43.1
		5	1182.2	7.4	39.5
		7.5	1174.8	5.93	35.2
		10	1166.4	4.34	31.5
4 a	70 CH ₄ + 30 H ₂ 0.0023 (kg/s)	0	1193	16.6	43.3
		2.5	1189.3	12.76	40.3
		5	1178.1	9.52	37.2
		7.5	1174.1	7.56	32.5
		10	1166.2	5.51	29
5 a	60 CH ₄ + 40 H ₂ 0.0021 (kg/s)	0	1193	23.6	42.9
		2.5	1185	17.9	39.2
		5	1178.9	13.3	35.1
		7.5	1173.9	10.5	32.3
		10	1167.1	7.84	26.5

due to the increased share of hydrogen in the fuel, the lowest fuel consumption is observed, owing to the higher heating value. Given that NO_x emissions are higher in this case compared to others, using humidified air is necessary to reduce NO_x levels. As observed, increasing the air humidity not only reduces NO_x emissions but also brings CO emissions to their minimum level.

8. CONCLUSION

This study provides a comprehensive three-dimensional simulation of wet combustion for a hydrogen-methane mixture in the annular combustion chamber of a microturbine. By employing the partially premixed combustion model and leveraging the $k-\epsilon$ Realizable turbulence model along with the probability density function (PDF) for chemical reactions, the research achieved significant insights into the effects of combustion humidification on emission reduction and combustion efficiency.

The study demonstrated that introducing humidity levels of 2.5%, 5%, 7.5%, and 10% in the inlet air significantly reduces pollutant emissions. Specifically, NO_x emissions decreased by 68% when the fuel mixture contained 10% hydrogen, with the maximum reduction

occurring at 10% humidity. Similarly, CO emissions were reduced by 48% for a fuel mixture containing 40% hydrogen under the same humidity level. This reduction is primarily due to the lowered peak combustion temperatures and the dilution effect, which slows the reaction rates responsible for NO_x formation. Additionally, a higher hydrogen content in the fuel mixture further contributed to emission control, with CO levels decreasing by as much as 16% when compared to methane alone, underscoring the benefits of hydrogen as a cleaner-burning fuel.

Moreover, combustion humidification led to a more uniform temperature distribution throughout the combustion chamber. This study, therefore, suggests that combining hydrogen fuel with wet combustion technology holds promise for advancing microturbines toward higher efficiency and reduced environmental impact. These findings highlight the potential for sustainable energy applications where reducing emissions and fuel consumption is a priority.

In summary, this research demonstrates the practical benefits of combustion humidification for reducing harmful emissions in microturbines. Further work may explore advanced combustion models and varied fuel

compositions to optimize these outcomes across diverse operational conditions.

CONFLICT OF INTEREST

This article is based on the first author's thesis conducted under the supervision of the second author, with no conflicts of interest to declare.

AUTHORS CONTRIBUTION

A. Sohrabi: conducting the research, performing simulations, and drafting. **M. Mirsajedi:** supervising the research, contributing to the study's conceptual framework, and providing guidance throughout the process. Both authors reviewed and approved the final manuscript.

REFERENCES

- Abagnale, C., Cameretti, M. C., De Robbio, R., & Tuccillo, R. (2017). Thermal cycle and combustion analysis of a solar-assisted micro gas turbine. *Energies*, 10(6), 773. <https://doi.org/10.3390/en10060773>
- Adamou, A., Costall, A., Turner, J. W., Jones, A., & Copeland, C. (2023). Experimental performance and emissions of additively manufactured high-temperature combustion chambers for micro-gas turbines. *International Journal of Engine Research*, 24(4), 1273-1289. <https://doi.org/10.1177/14680874221082636>
- Banerjee, A., Sarkar, S., Mukhopadhyay, A., & Sen, S. (2021). *The effects of steam and water spray addition on NOx emissions from a combustor using simple reactor models*. Conference on Fluid Mechanics and Fluid Power. https://doi.org/10.1007/978-981-19-6970-6_87
- Bastani, M., Tabejamaat, S., Mani, M., & Ashini, H. (2025). Numerical and experimental investigation of microturbine combustion chamber performance and emissions through biogas consumption with varied component ratios. *Fuel*, 380, 133234. <https://doi.org/10.1016/j.fuel.2024.133234>
- Bolszo, C., & McDonell, V. (2009). Emissions optimization of a biodiesel fired gas turbine. *Proceedings of the Combustion Institute*, 32(2), 2949-2956. <https://doi.org/10.1016/j.proci.2008.07.042>
- Bouam, A., Aissani, S., & Kadi, R. (2008). Combustion chamber steam injection for gas turbine performance improvement during high ambient temperature operations. <https://doi.org/10.1115/1.2898834>
- Bulat P., V., Vokin Leonid, O., Konstantin, N. V., Nikitenko Alexander, B., Prodan Nikolai, V., & Maksim, E. R. (2024a). Configurable combustion models of combustion chamber of microturbine engine with possibility of connecting various physico-chemical processes. *Journal Scientific and Technical Of Information Technologies, Mechanics and Optics*, 156(4), 645. <https://doi.org/10.17586/2226-1494-2024-24-4-645-653>
- Bulat, P., Vokin, L., Volkov, K., Nikitenko, A., Prodan, N., & Renev, M. (2024b). Numerical simulation of performance of micro gas turbine engine combustion chamber taking into account oil addition to fuel. *Russian Aeronautics*, 67(3), 594-600. <https://doi.org/10.3103/S1068799824030140>
- Caldeira-Pires, A., Heitor, M., & Carvalho Jr, J. (2000). Characteristics of nitric oxide formation rates in turbulent nonpremixed jet flames. *Combustion and Flame*, 120(3), 383-391. [https://doi.org/10.1016/S0010-2180\(99\)00094-2](https://doi.org/10.1016/S0010-2180(99)00094-2)
- Cameretti, M. C. (2020). Modelling of a hybrid solar micro-gas turbine fuelled by biomass from agriculture product. *Energy Reports*, 6, 105-116. <https://doi.org/10.1016/j.egy.2019.10.026>
- Carusotto, S., Goel, P., Baratta, M., Misul, D. A., Salvadori, S., Cardile, F., Forno, L., Toppino, M., & Valsania, M. (2022). Combustion characterization in a diffusive gas turbine burner for hydrogen-compliant applications. *Energies*, 15(11), 4117. <https://doi.org/10.3390/en15114117>
- Chen, J., Mitchell, M. G., & Nourse, J. G. (2009). *Development of ultra-low emission liquid fuel-fired microturbine engines for vehicular heavy duty applications*. Turbo Expo: Power for Land, Sea, and Air. <https://doi.org/10.1115/GT2009-60257>
- Chen, J., Mitchell, M. G., & Nourse, J. G. (2010). *Development of ultra-low emission diesel fuel-fired microturbine engines for vehicular heavy duty applications: combustion modifications*. Turbo Expo: Power for Land, Sea, and Air, <https://doi.org/10.1115/GT2010-23181>
- Chen, S., Zhao, D., Li, H. K. H., Ng, T. Y., & Jin, X. (2017). Numerical study of dynamic response of a jet diffusion flame to standing waves in a longitudinal tube. *Applied Thermal Engineering*, 112, 1070-1082. <https://doi.org/10.1016/j.applthermaleng.2016.10.152>
- De Robbio, R. (2017). Innovative combustion analysis of a micro-gas turbine burner supplied with hydrogen-natural gas mixtures. *Energy Procedia*, 126, 858-866. <https://doi.org/10.1016/j.egypro.2017.08.291>
- De Soete, G. G. (1975). *Overall reaction rates of NO and N2 formation from fuel nitrogen*. Symposium (international) on combustion. [https://doi.org/10.1016/S0082-0784\(75\)80374-2](https://doi.org/10.1016/S0082-0784(75)80374-2)
- Di Nardo, A., Bo, A., Calchetti, G., Giacomazzi, E., & Messina, G. (2020). Study on the fuel flexibility of a microgas turbine combustor burning different mixtures of H2, CH4, and CO2. *Journal of Engineering for Gas Turbines and Power*, 142(6), 061001. <https://doi.org/10.1115/1.4046706>
- Du Toit, M., Engelbrecht, N., Oelofse, S. P., & Bessarabov, D. (2020). Performance evaluation and emissions reduction of a micro gas turbine via the co-

- combustion of H₂/CH₄/CO₂ fuel blends. *Sustainable Energy Technologies and Assessments*, 39, 100718. <https://doi.org/10.1016/j.seta.2020.100718>
- Fafara, J. M. (2025). CFD study case of ammonia-hydrogen mixture powered methane gas microturbine combustor in the context of the temperature repartition modifications. *Combustion Engines*. <https://doi.org/https://doi.org/10.19206/CE-197220>
- Fantozzi, F., Laranci, P., Bianchi, M., De Pascale, A., Pinelli, M., & Cadorin, M. (2009). *CFD simulation of a microturbine annular combustion chamber fuelled with methane and biomass pyrolysis syngas: Preliminary results*. Turbo Expo: Power for Land, Sea, and Air. <https://doi.org/10.1115/GT2009-60030>
- Farokhipour, A., Hamidpour, E., & Amani, E. (2018). A numerical study of NO_x reduction by water spray injection in gas turbine combustion chambers. *Fuel*, 212, 173-186. <https://doi.org/10.1016/j.fuel.2017.10.033>
- Fatehi, M., Campaldini, G., & Renzi, M. (2025). Micro gas turbine fed by ammonia with steam injection: Performance and combustion analysis. *Applied Thermal Engineering*, 125428. <https://doi.org/https://doi.org/10.1016/j.applthermaleng.2025.125428>
- Fluent, A. (2011). Ansys fluent theory guide. *Ansys Inc., USA*, 15317, 724-746.
- Funke, H. W., Beckmann, N., & Abanteriba, S. (2019). An overview on dry low NO_x micromix combustor development for hydrogen-rich gas turbine applications. *International Journal of Hydrogen Energy*, 44(13), 6978-6990. <https://doi.org/10.1016/j.ijhydene.2019.01.161>
- Furuhata, T., Kawata, T., Mizukoshi, N., & Arai, M. (2010). Effect of steam addition pathways on NO reduction characteristics in a can-type spray combustor. *Fuel*, 89(10), 3119-3126. <https://doi.org/10.1016/j.fuel.2010.05.018>
- Glanville, P., Fridlyand, A., Sutherland, B., Liszka, M., Zhao, Y., Bingham, L., & Jorgensen, K. (2022). Impact of hydrogen/natural gas blends on partially premixed combustion equipment: NO_x emission and operational performance. *Energies*, 15(5), 1706. <https://doi.org/https://doi.org/10.3390/en15051706>
- Haynes, J., Janssen, J., Russell, C., & Huffman, M. (2006). *Advanced combustion systems for next generation gas turbines*. <https://doi.org/10.2172/888744>
- Jamshidiha, M., Kamal, M., Cafiero, M., Coussement, A., & Parente, A. (2024). Experimental and numerical characterization of hydrogen combustion in a reverse-flow micro gas turbine combustor. *International Journal of Hydrogen Energy*, 55, 1299-1311. <https://doi.org/https://doi.org/10.1016/j.ijhydene.2023.11.243>
- Khosravy el_Hossaini, M. (2013). *Review of the new combustion technologies in modern gas turbines*. Progress in Gas Turbine Performance, 978-953. <https://doi.org/10.5772/54403>
- Lefebvre, A. H., & Ballal, D. R. (2010). *Gas turbine combustion: alternative fuels and emissions*. CRC press. <https://doi.org/10.1201/9781420086058>
- Lellek, S., Barfuß, C., & Sattelmayer, T. (2017). Experimental study of the interaction of water sprays with swirling premixed natural gas flames. *Journal of Engineering for Gas Turbines and Power*, 139(2), 021506. <https://doi.org/10.1115/1.4034238>
- Lu, J., Fu, Z., Liu, J., & Pan, W. (2022). Influence of air distribution on combustion characteristics of a micro gas turbine fuelled by hydrogen-doped methane. *Energy Reports*, 8, 207-216. <https://doi.org/10.1016/j.egy.2021.11.027>
- Medhat, M., Yehia, M., Franco, M. C., & Rocha, R. C. (2021). A numerical prediction of stabilized turbulent partially premixed flames using ammonia/hydrogen mixture. *Journal of Advanced Research in Fluid Mechanics and Thermal Sciences*, 87(3), 113-133. <https://doi.org/10.37934/arfmts.87.3.113133>
- Meziane, S., & Bentebbiche, A. (2019). Numerical study of blended fuel natural gas-hydrogen combustion in rich/quench/lean combustor of a micro gas turbine. *International Journal of Hydrogen Energy*, 44(29), 15610-15621. <https://doi.org/10.1016/j.ijhydene.2019.04.128>
- Nam, J., Lee, Y., Joo, S., Yoon, Y., & Yoh, J. J. (2019). Numerical analysis of the effect of the hydrogen composition on a partially premixed gas turbine combustor. *International Journal of Hydrogen Energy*, 44(12), 6278-6286. <https://doi.org/10.1016/j.ijhydene.2019.01.066>
- Pappa, A., Bricteux, L., Bénard, P., & De Paepe, W. (2021). Can water dilution avoid flashback on a hydrogen-enriched micro-gas turbine combustion?—a large eddy simulations study. *Journal of Engineering for Gas Turbines and Power*, 143(4), 041008. <https://doi.org/10.1115/1.4049798>
- Patankar, S. (2018). Numerical heat transfer and fluid flow. <https://doi.org/https://doi.org/10.1201/9781482234213>
- Poinsot, T., & Veynante, D. (2005). *Theoretical and numerical combustion*. RT Edwards, Inc.
- Reale, F. (2022). Effects of steam injection on the permissible hydrogen content and gaseous emissions in a micro gas turbine supplied by a mixture of CH₄ and H₂: A CFD analysis. *Energies*, 15(8), 2914. <https://doi.org/10.3390/en15082914>
- Reale, F., & Sannino, R. (2021). Water and steam injection in micro gas turbine supplied by hydrogen enriched fuels: Numerical investigation and performance analysis. *International Journal of Hydrogen Energy*, 46(47), 24366-24381. <https://doi.org/10.1016/j.ijhydene.2021.04.169>

- Reale, F., Calabria, R., Chiariello, F., Pagliara, R., & Massoli, P. (2012). A micro gas turbine fuelled by methane-hydrogen blends. *Applied Mechanics and Materials*, 232, 792-796. <https://doi.org/10.4028/www.scientific.net/AMM.232.792>
- Serbin, S., Burunsuz, K., Chen, D., & Kowalski, J. (2022). Investigation of the characteristics of a low-emission gas turbine combustion chamber operating on a mixture of natural gas and hydrogen. *Polish Maritime Research*, 29(2), 64-76. <https://doi.org/10.2478/pomr-2022-0018>
- Shan, F., Zhang, D., Hou, L., Fang, H., & Zhang, H. (2022). Partially premixed combustion simulation using a novel transported multi-regime flamelet model. *Acta Astronautica*, 191, 245-257. <https://doi.org/https://doi.org/10.1016/j.actaastro.2021.11.020>
- Sher, A. A., Ahmad, N., Sattar, M., Phelan, P., & Lin, A. (2024). Computational analysis of multi-fuel micro-gas turbine annular combustion chamber. *Journal of Thermal Analysis and Calorimetry*, 149(8), 3317-3329. <https://doi.org/https://doi.org/10.1007/s10973-024-12924-z>
- Shih, H. Y., & Liu, C. R. (2014). A computational study on the combustion of hydrogen/methane blended fuels for a micro gas turbines. *International Journal of Hydrogen Energy*, 39(27), 15103-15115. <https://doi.org/10.1016/j.ijhydene.2014.07.046>
- Sohrabi, A., & Mirsajedi, S. M. (2024). 3D simulation and study of biogas combustion in C30 microturbine annular combustion chamber. *Fuel and Combustion*, 17(1), 72-86. <https://doi.org/10.22034/jfnc.2024.456905.1392>
- Therkelsen, P., Mauzey, J., McDonell, V., & Samuelsen, S. (2006). *Evaluation of a low emission gas turbine operated on hydrogen*. Turbo Expo: Power for Land, Sea, and Air. <https://doi.org/10.1115/GT2006-90725>
- Therkelsen, P., Werts, T., McDonell, V., & Samuelsen, S. (2009). Analysis of NOx formation in a hydrogen-fueled gas turbine engine. *Journal of Engineering for Gas Turbines and Power*, 131(3). <https://doi.org/10.1115/1.3028232>
- Wang, P., Hashemi, S. M., He, H., & Cheng, K. (2022). Investigation of the partially premixed turbulent combustion through the PRECCINSTA burner by large eddy simulation. *Aerospace Science and Technology*, 121, 107336. <https://doi.org/https://doi.org/10.1016/j.ast.2022.107336>
- Xiao, C., Omid, M., Surendar, A., Alizadeh, A. a., Bokov, D. O., Binyamin, & Toghraie, D. (2022). Simulation of combustion flow of methane gas in a premixed low-swirl Burner using a partially premixed combustion model. *Journal of Thermal Science*, 31(5), 1663-1681. <https://doi.org/https://doi.org/10.1007/s11630-022-1611-z>